Physico-chemical characterization of snail shells powder prepared by mechanochemical processes and thermal treatment

Mostapha KARAOUI[1,*], Rachid HSISSOU[2], Mohammed ALAMI[1], and Mohammed ASSOUAG[1]

[1] *Team of Innovative Materials and Mechanical Manufacturing Processes, ENSAM, University Moulay Ismail, B.P. 15290, Al Mansour, Meknes, Morocco*

[2] *Laboratory of Organic Chemistry, Catalysis and Environment. Department of Chemistry, Faculty of Sciences, Ibn Tofail University, BP 242, 14000 Kenitra, Morocco*

*Corresponding author e-mail: most.karaoui@edu.umi.ac.ma

Abstract

   Natural particles are the most abundant resources exist in nature. Bio-sources of $CaCO_3$ particles have attracted the attention of researchers for multiple cosmetics, industrial, and medical applications. This work investigates the structural evolution of $CaCO_3$ containing in *snail shell* particles prepared by a mechanochemical process using methods of characterization as well as Differential scanning calorimeter (DSC), Thermogravimetric analysis (TGA), X-ray diffraction (X-RD), Fourier transformation infra-red (FT-IR), and Scanning microscopy equipped with Energy-dispersive X-Ray spectroscopy (SEM-EDXS). The result obtained from the above analysis indicates that SSP calcined between 200℃ to 400℃ undergoes an elimination of water molecules, followed by a phase transformation from Aragonite to $CaCO_3$ Calcite. At 800℃, the SSP decomposes $CaCO_3$, giving rise to calcium oxide crystals CaO, which release CO_2 molecules. These eliminations and transformations represent a loss of 47.08% of the initial mass at 800℃. The morphological analysis shows the surface of SSP calcined at 800℃ with $CaO/CaCO_3$ crystal formation. Also, the mechanochemical process leads to obtaining an SSP with a size between 3.311 μm to 10.140 μm. *Snail shells* can be a natural source of $CaCO_3$ and CaO, thanks to their ease of extraction and processing.

1. Introduction

   Snail shell is one of the most abundant constituents of our household waste. The potential of this waste has not yet been fully exploited. Based on the recovery and reuse of biological resources, the use of *snail shells* has increased slightly in recent years [1]. Due to their high availability and low cost, the identification and characterization of snail shell particles of different sizes have drawn the attention of researchers and scientists in several areas. Jankovic *et al.* and Rujitanapanich *et al.* [2,3] report a new procedure for synthesizing hydroxyapatite from the *oyster shell* by precipitation. In addition, they have been studies to use it as a CO_2 sorbent after characterization [4]. Another study evaluates the feasibility of using *snail shells* from industrial waste to remove copper ions Cu^{2+}. This study is based on the effect of thermal pretreatment in the range of 300℃ to 900℃ on the adsorption of copper ions [5]. Also, studies have been done on the kinetics of wastewater treatment in the brewing industry using *snail shell* particles [6].

   Other studies focused on the thermal treatment and characterization of *snail shells* obtained by mechanochemical grinding techniques to reinforce epoxy polymer matrices. The results have confirmed that mechanochemical grinding avoids and inhibits the formation of agglomerations of the *snail shell* particles keeping the obtained nanometric size and also the excellent distribution of the particles in the epoxy polymer [7,8] The same aspect of using *snail shells* as reinforcement of polyester matrix for coating the surface of steels against corrosion has also been evaluated by [9]. Calcium carbonates are among the essential things in our daily life, and it exists in four forms amorphous $CaCO_3$, Aragonite, vaterite, and calcite polymorph. Calcium oxide crystals CaO formed due to the carbonation of $Ca(OH)_2$ without an organic substrate [10]. The major difference between the *snails* and *eggs shell* is in their composition, the *eggs shell* is rich in calcite, and when chemical treatment is made, they form calcium oxide phases [11]. While the *snail shell* is rich in aragonite, transforms to calcite polymorph, decomposes to calcium oxide, and liberates carbon dioxide [4,11]. The structure of the *snail shell* is constituted mainly of 3 layers. The first is the Periostracum, the external organic layer of the *shell*. The second is the *Calcareous* layer called *Ostracum*, and the third is the *Hypostracum*, the internal calcareous layer of the shell. It can be either round or conical, smooth or textural. It also can be uncoloured, fasciated, spotted, or mottled. However, the bands can be vertical, horizontal, zigzagged, or diagonal [12]. The size of the particles plays a critical role due to their physicochemical properties. Again, the smaller particles have a larger surface area-to-volume ratio, which means that a more significant proportion of the particles is exposed to the surrounding environment. As a result, smaller particles

tend to have a higher reactivity and a greater susceptibility to chemical reactions, transformation, and thermal degradation. A study investigated the reinforcing properties of nano-$CaCO_3$ synthesized from the *snail shell Achatina Fulica* by mechanochemical methods on epoxy nanocomposites. They found that ethanol is a suitable solvent for wet milling. In addition, it allows reaching nanoparticles in the range of 13.48 nm to 42.90 nm [7,13]. Karaoui *et al*. [14], use this snail shell elaborated by mechanochemical process and heat treated as reinforcement to polystyrene polymer matrice. The result confirmed that the micrometric particles SSP elaborated enhance the thermal, flow, and mechanical properties of the composites formed (PS/SSP). The aim of this study is first, the preparation by crushing *snail shell* using a mechanochemical process, then sieving of the powder obtained to a size of 63 μm. To better understand the transformation and the eliminations undergone from the powder of *snail shell* during the process of calcination at the range of temperatures of 200, 400, 500, 600, 700, 800, and 900°C, many analyses and characterizations of the powder were made using Thermogravimetric analysis (TGA-DTG) and Differential scanning calorimeter (DSC), X-ray diffraction (X-RD), Fourier transformation infra-red (FT-IR), and Scanning microscopy equipped with energy-dispersive x-ray spectroscopy (SEM-EDXS).

2. Experimental

2.1 Solvent and material

The snail shell was collected from restaurants as consumers' waste products and from vendors. The ethanol (99.9% purity) used in the wet milling was supplied by Biosmart (Biosmart, Casablanca, Morocco).

2.2 Preparation of snail shell particles

The Achatina fulica of snail shell was collected from vendors in the Meknes region, Morocco. The preparation process of $CaCO_3$ particles was carried out in our laboratory. It is necessary to wash and disinfect the snail shell using distilled water and chlorine bleach (NaHClO). The snail shell was washed and rinsed with distilled water several times and kept at room temperature for 24 h to dry before being ground, then grinding was done with a ball milling using the single planetary grinder PULVERISETTE 6 classic line (Fritsch GmbH, Germany), with the speed of 450 rpm, for 30 min. The powder obtained was sieved to a diameter of 63 μm using a vertical vibratory sieve shaker (Fritsch Analysette 3 Spartan, Fritsch, Germany) under 50 Hz to 60 Hz and a power of 50 W. The mechanochemical milling process was carried out according to the method mentioned in the literature, using ethanol as a solvent [7,13-15]. The physico-chemical properties of the snail shell obtained after the processes mentioned above are cited in Table 1.

2.3 Thermal Analysis

2.3.1 Thermal treatment

The heat treatment of the snail shell particles obtained after dry and wet grinding was done using an electric furnace supplied by the MCC control Lab. The treatment temperatures were 200, 400, 500, 600, 700, 800, and 900°C for 4 h. The weight loss measurements were weighed using a balance (BEL ENGINEERING, LCD Display, ITALY) with an uncertainty of 0.0001 g.

2.3.2 Differential Scanning Calorimeter (DSC)

Thermogravimetric analysis, with derivative Thermogravimetry (TGA-DTG) and Differential scanning calorimeter (DSC), are among the most common techniques for determining the thermal characteristics of snail shell particles. It was performed to complement the mineralogical and structural information derived from the snail shell particles. This study evaluated thermal measurements using the LABSYS evo (SERTARAL Instrumentation KEP technologies group, USA) instrument machine. The sample containing 21.6 mg of raw SSP was put into an aluminium pan and characterized at a temperature ramp of 10°C·min^{-1} from 20°C to 1000°C.

2.4 Spectroscopic Analysis

2.4.1 FT-IR Analysis

A Fourier transform infrared spectrophotometer (FT-IR) analysis using a Bruker Alpha-II FT-IR (Bruker, Billerica, Massachusetts, USA) instrument to evaluate the functional groups of raw SSP and calcined at different temperatures from 200°C to 800°C. The spectra were registered in the attenuated total reflectance (ATR) range of 400 cm^{-1} to 4000 cm^{-1} with 24 scans and a resolution of 4 cm^{-1}.

2.4.2 XRD Analysis

X-ray diffraction (X-RD) techniques are among the most important tools for materials characterization. The X-ray diffraction spectra were performed with a powder diffractometric (Model D8 Advance Bruker, Billerica, Massachusetts, USA) equipped with a copper anode tube monochromatic source. The radiation used is the Cu-Kα (λ=1.54 Å). The spectra were recorded at room temperature. The recording conditions are tube current and an applied voltage of 40 mA and 40 kV, respectively. The diffraction patterns were recorded from 10° to 90° (2θ) with continuous scanning at a step size of 0.017 (2θ) and a scan step time of 192 s.

2.4.3 SEM & EDXS Analysis

The scanning microscopy equipped with energy-dispersive X-ray spectroscopy (EDXS) operated under a high vacuum mode (JSM-IT500HR, USA) was used to observe the morphology and to evaluate the elemental composition of raw SSP at different temperatures.

Table 1. Physical-chemical characterization of SSP.

Properties	*Snail shell* particle
Granulometry (μm)	< 63
The apparent density (g·cm^{-3})	0,9545
The specific surface (m^2·g^{-1})	0,099
Humidity (%)	1,075
Ash content (%)	4,85

3. Result and discussion

3.1 Thermal treatment

3.1.1 Visual aspect

Raw snail shell particles (SSP) obtained are presented in Figure 1(E). It is a rough white-beige powder, less than 63 µm in size. The visual aspect of the calcined derivative particles of the snail shell shows in Figure 1. The colours in the first states of the snail shell vary from the white-brown (A-B-C) to beige (D) and white-beige (E-F) in size under 75 and 63µm, respectively. We notice that the increase in temperature causes changes in the colour of snail shell particles from white-beige (E-F) at 200°C to white (G) at 400°C. Perhaps these changes are caused by the evaporation of adsorbed water. The colour-changing in the temperature range from 500°C to 600°C is due to the beginning of the carbonization of SSP. Finally, we observe that the colour in (J) changed from white-grey to pure white (K), (L) at 700, 800, and 900°C, respectively. We can say that the white colour appeared thanks to the SSP calcined in the state (K-L) and remained stable in temperatures 800°C and 900°C. Therefore, we suggest it was due to a change in the treated SSP's composition and morphology [11].

3.1.2 Weight loss

The weight loss of our powder during the thermal treatment is presented in Figure 2. It shows two distinct parts of the weight loss: one at a temperature below 600°C and the other from 650°C to 900°C. The first part can be explained by releasing hygroscopic water below 120°C, water in hydrated salts between 120°C to 200°C [16], and water linked to carbonates between 200°C and 400°C. Also, the decarbonization of calcium carbonate and elimination of chemically bound water and organic matter between 400°C to 650°C. In addition to transforming aragonite to calcite polymorphs [17,18]. The second part of weight losses is due to the endothermic decomposition of $CaCO_3$ to CaO in a range of 650°C to 900°C, which could be confirmed by X-ray diffraction (X-RD) and Differential scanning calorimeter (DSC). This decomposition was accompanied by a release of CO_2 [4].

3.1.3 Differential scanning calorimeter DSC

This analysis study used the differential scanning calorimeter (DSC) and Thermogravimetric analysis with Derivative thermo-gravimetry (TGA-DTG) to know the weight loss and heat flow during the phase's transformation of snail Shell in a temperature from 20°C to 1000°C. Figure 3 shows the TGA-DTG/DSC thermogram obtained. The TGA shows the weight loss of SSP as a function of temperature. We can see from the thermogram that it's composed of many processes.

The weight loss of the SSP is represented in the thermogram TGA-DTG in milligrams and percentages compared to the initial mass. The first losses appear at around 198.64°C with a rate of 2.54% due to the drying of the SSP by leaving the water molecules. In addition, at a temperature of 380°C, a loss with a percentage of 7.8% was detected, caused by the removal of organic compounds from the snail shell and the water molecules linked to the aragonite molecules,

caused by the beginning of the snail shell carbonization by changing its colour from white to grey. The second part of the losses around the temperature of 551.42°C with a percentage of 12.91%, related to the transformation process of the aragonite phases into calcite. This is followed by a percentage loss of 13.61% with a temperature of 694.88°C. The significant loss of the snail shell mass is at a temperature of about 796.4°C with a percentage loss of 47.08%. Furthermore, this weight loss confirms the result obtained in the visual aspect by a change in the colour of snail shell particles thermally treated. Table 2 compares temperatures and percentages of significant snail shell loss with other works. The results obtained are coherent with Shafu Kamba *et al.* [19], Egreric *et al.* [5], and Redouane *et al.* [11]. In the same sense, Fombuena *et al.* [20], found the weight loss of shellfish from different mollusks close to 42% at 817°C. Also, Egeric *et al.* [5] have reported a decrease of 45.1% at 900°C. In addition, Redouane *et al.* [11] studied and characterized Moroccan snail shells and found that the significant loss is situated at a temperature of 835°C with a percentage of 40.18%. They found that these materials have a conversion rate of 0.6 g CaO/g $CaCO_3$. The conversion rate found is 0.53 g CaO/$CaCO_3$.

Figure 1. The visual aspect of snail shell, SSP, and different compounds obtained after milling and heat treatment at temperatures ranging from 200 to 900°C.
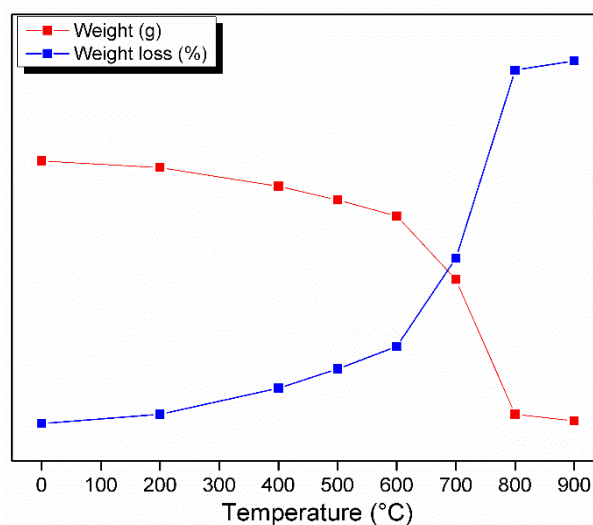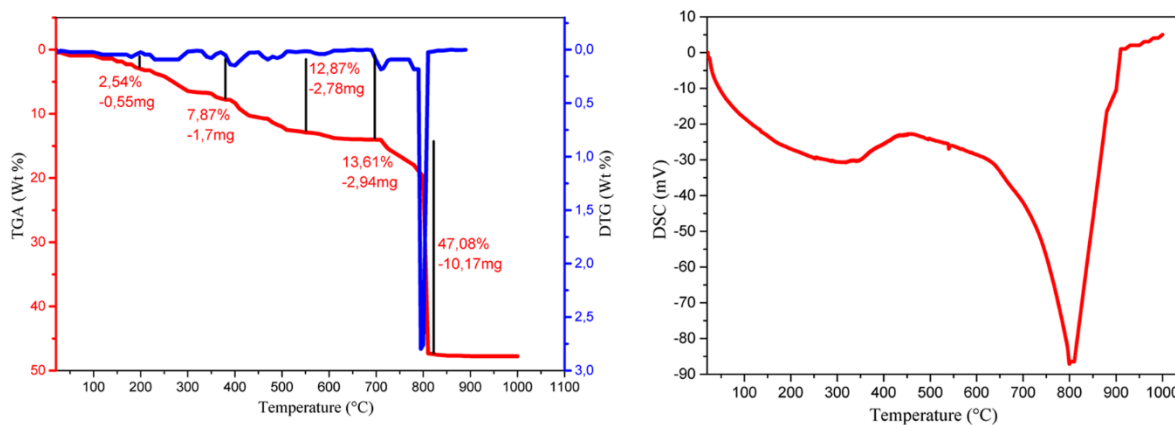

Figure 2. Mass loss of SSP at different temperatures.

Table 2. Comparison of temperature and percentage of decomposition of snail shell into CaO.

Decomposition to CaO	Temperature (°C)	Percentage of loss (%)	Reference
Snail shell	796.4	47.08	Present work
Snail shell	835	40.18	[11]
Seashell	817	42	[20]
Snail shell	900	45.1	[5]
Mussel shell	631-765	41.3	[21]

Figure 3. TGA-DGT/DSC curves of SSP in a range of 20°C to 800°C.

Other work by Hu *et al*. [21] reported a significant weight reduction of 41.3% in a freshwater *mussel shell* when the temperature was increased from 631°C to 765°C. Also, when the calcination temperature exceeds 800°C, the weight loss remains almost constant until it reaches 830°C. As a result, the appropriate calcination temperature for decomposing $CaCO_3$ to CaO is lower than 830°C. The results show the decomposition of $CaCO_3$ to CaO by releasing the CO_2 molecules. Moreover, the results obtained are similar to those of the weight loss measurement.

The DSC represents the heat flux absorbed or given off during a transformation or loss of the compounds in the *snail shell* particles (Figure 3). A large endothermic peak around 200°C to 390°C is attributed to the dehydration of the *snail shell*; it is the release of free water molecules bound to the SSP compounds. Also, the decomposition of organic matter that remains in the *snail shell* after the washing and cleaning process [22]. The exothermic peak of about 450°C to 560°C is due to the transformation of aragonite phases into calcite. It was passing from an orthorhombic crystalline phase to another rhombohedric one. The large endothermic peak from 790°C indicates the beginning of the decomposition of the calcite phases $CaCO_3$ into Calcium oxide CaO with a release of CO_2 molecules that RD-X and IR-TF analysis can confirm [19,23,24]. It is found that mechanochemical grinding affects the particle size since it results in fine particles of micrometric size.

Consequently, the size influences the transformation and decomposition temperatures found in our work compared to works in the literature. Also, the decrease in the size of the prepared SSP increases their surface and reactivity with the external environment, leading to the transformation of polymorphs and release of carbon dioxide CO_2 from the conversion of calcite to calcium oxide CaO. The value found is 47.08% in comparison with other works. Therefore, the transformations and decomposition are easier and do not absorb more energy and temperature, contrary to other works mentioned in Table 2 [7,13,15]. In addition to the highest value of the conversion

rate, which represents the amount of $CaCO_3$ transformed into CaO. In other words, the mechanochemical process allows us to fine particles of a micrometric size that positively influence the transformations and decomposition of $CaCO_3$ contained in the *snail shell*. The SEM analysis can confirm the size of these particles.

3.2 Spectroscopic analysis

3.2.1 FT-IR

Fourier transform-infrared spectroscopy (FT-IR) instrument analyses the *snail shell* powder before and after calcination at different temperatures. This technique allowed us to identify adsorption bands corresponding to the various vibrations bands characteristic of the phases in the material surface.

Figure 4 shows the infrared spectra of raw SSP and SSP powder calcined at different temperatures from 200°C to 800°C. The values of absorption bands are represented in Table 3. The principal SSP bands are observed at 1455.55, 1083.88, and 855.17 cm^{-1}, and a double peak at 712.22 cm^{-1} and 702.5 cm^{-1}. The FT-IR spectrum of the raw SSP shows the presence of a fundamental vibration mode characteristic of carbonate ion (CO_3^{-2}). It is identified by the major absorption bands of 1455.55, 1083.88, 855.17, and 712.22 cm^{-1}. The infrared spectra of SSP and SSP calcined at 200°C show double peaks at 712.22 cm^{-1} and 702.50 cm^{-1}, characteristic of polymorphic $CaCO_3$ Aragonite.

In contrast, the treatment of raw SSP at 400, 500, and 600°C shows a single bond at 712.22 cm^{-1}. This is a characteristic of polymorphic calcite $CaCO_3$. The results completely agree with the studies mentioned in [11,25]. FT-IR of SSP calcined at 400°C to 600°C shows three strong absorption bands at 1392.35, 855.12, and 712.22 cm^{-1}. These bands indicate the presence of CO_3^{-2} bound to Ca^{2+} in the calcite structure. They also correspond to asymmetric in-plane expansion and contraction and bending vibration modes of C--O bonds in calcite [26].

Table 3. Major pics of raw SSP and calcined at different temperatures from 200°C to 800°C.

	Raw SSP and calcined at 200°C	SSP calcined at 400 to 600°C	SSP calcined 700 and 800°C
Compound	Aragonite	Calcite	Calcite - Calcium Oxide
Formula	$CaCO_3$	$CaCO_3$	$CaCO_3$ - CaO
FT-IR Bands	702,5	712,22	508
	712,22	855,17	712,22
	855,17	1392,35	855,17
	1083,88	1386,30	1392,35
	1455,55	1420,94	3643,40

The intensity of the peak corresponding to the $CaCO_3$ Calcite/ Aragonite absorption band decreased by 800°C in the FT-IR spectrum of the calcinated SSP. In the FT-IR spectrum of SSP calcinated above 700°C, new absorption bands appeared at 3639.50 cm^{-1} and 501 cm^{-1}. They are due to the vibrations of Ca--O and aragonite. They are due to the vibration of Ca---OH bonds of Ca $(OH)_2$ and Ca--O bonds of CaO [26].

Biogenic $CaCO_3$ decomposes to CaO during calcination at temperatures above 700°C and then hydrates to Ca $(OH)_2$ under ambient conditions [12]. The hygroscopic properties of CaO make their activation energy low which prevents reaction with H_2O to form Ca $(OH)_2$ according to the following reaction R-1 [11]:

$$CaO_{(s)} + H_2O_{(g)} \rightarrow Ca(OH)_{2\,(s)} \qquad R\text{-}1$$
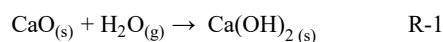
The main characteristic absorption bands of SSPs calcined at 800°C were observed at peaks 3634.40, 1391.25, and 855.17 cm^{-1}. These bands were similar to those of commercial CaO reported by Rujitanapanich *et al.* [3], the decrease in intensity of the peaks around 1455.55, 1420.94, and 1083.88 cm^{-1}, in addition to the appearance of new peaks around 3643.40 cm^{-1}, indicates and confirms the transformations and decompositions supposed during the thermal treatment from 200°C to 800°C. The result obtained supports the explanation posed in visual aspects and thermal treatment. Indeed, similar results are obtained and cited by [11,26].

3.2.2 X-ray diffraction Analysis

X-ray diffraction (XRD) is the technique that provides information regarding the structural and physical properties of crystalline samples including [1]. The structural transformation of *snail shells* at different temperatures has been investigated in previous studies [1,11,26-28].

The raw and calcined SSP data at different temperatures are shown in Figure 5. The raw SSP and calcined at 200°C represent different peaks in a range of 2Θ (25° to 55°), indicating the presence of aragonite phase crystalline. Aragonite is the metastable form of $CaCO_3$ at atmospheric pressure and ambient temperature [11]. Maximum major peaks are observed at 26.34, 27.48, 33.40, 36.3155, and 46.1187° for raw SSP, indicating the existence of $CaCO_3$ with aragonite crystalline form. Also, other peaks as 27.48, 36.3155, 38.6794, 48.5868, and 53,1755°. According to the international center of data diffraction, these peaks indicate the phase Aragonites crystalline with an *orthorhombic* form of $CaCO_3$ [29].

The temperature range 400°C to 600°C contains many peaks in Table 4. It can be seen that as the calcination temperature increases, the height of the $CaCO_3$ peaks decreases, and the appearance of new

peaks of the $CaCO_3$ calcite form. This new polymorph of calcite indicates the physical transformation of aragonites to calcite phases with a *rhombohedric* form of $CaCO_3$, according to the reaction mentioned in the literature R-2 [5,28].

$$CaCO_{3(Aragonite)} \rightarrow CaCO_{3\,(Calcite)} \qquad R\text{-}2$$
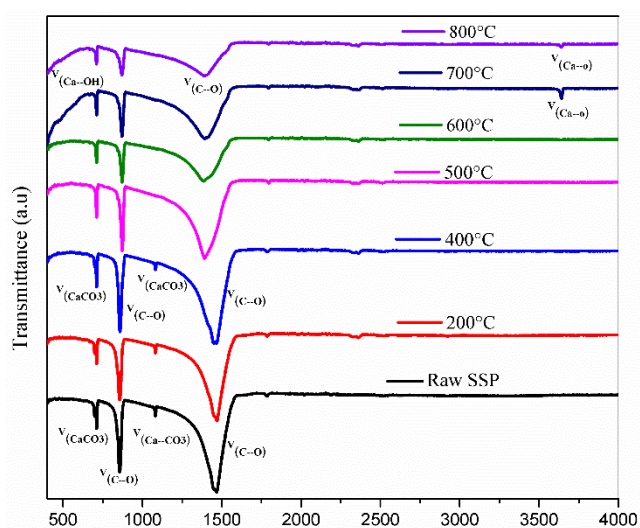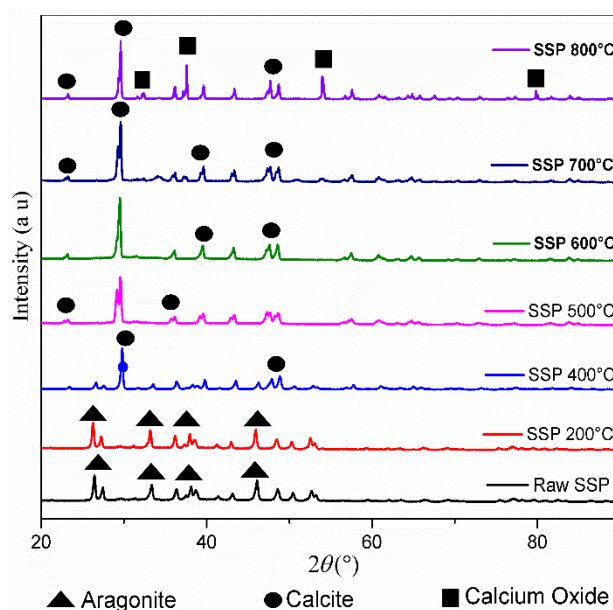

Figure 4. Infrared spectra of SSP before and after calcination at different temperatures.

Figure 5. XRD Analysis of raw SSP, and calcined at different temperatures.

Table 4. Different chemical compounds of raw SSP and calcined at different temperatures.

	Raw-200°C	SSP 400 - 600°C	SSP 700°C		SSP 800°C	
Compound Name	Aragonite	Calcite	Calcite	Calcium Oxide	Calcite	Calcium Oxide
Formula	$CaCO_3$	$CaCO_3$	$CaCO_3$	CaO	$CaCO_3$	CaO
Crystal System	Orthorhombic	Rhombohedral	Rhombohedral	Cubic	Rhombohedral	Cubic
Space group	Pmcn	R-3c	R-3c	Fm3m	R-3c	Fm3m
Space group number	62	167	167	225	167	225
2Θ (°)	26,3490	23,2476	23,2476	37,3793	23,2476	37,5841
	27,3291	26,6269	29,6551	47,6928	29,6551	53,9979
	33,2685	29,4503	36,2821	48,6729	36,1797	57,6844
	36,2236	33,5464	39,6614		39,6614	60,8296
	37,9205	36,1797	43,3479		43,3479	67,6760
	43,0114	39,5444	47,6928		47,6927	79,8474
	45,9665	43,2455	48,6729		48,7753	83,9728
	48,5120	46,2592				53,9979
	50,3406	47,5757				57,6844
	52,6081	48,5560				
	53,0323	57,4649				
		60,8296				
		64,7502				

The aragonite phase is thermodynamically unstable compared to the calcite phase. The transformation of calcite to aragonite at high temperatures and ambient conditions is impossible [30].

In The increase of thermal temperature of SSP to 700°C, one notes an appearance of the peaks starting from 700°C with weak intensity. Indicating the beginning of the transformation of the crystalline phases of calcite $CaCO_3$ to the crystalline phases of calcium oxide CaO with the *cubic* form according to the reaction R-3 [25].

$$CaCO_3 \rightarrow CaO + CO_2 \qquad \text{R-3}$$

Calcium oxide is cited as the most stable phase thermodynamically in ambient conditions [28]. The peaks obtained are mentioned in Table 3. Above 700°C, we clearly show the appearance peaks of calcium oxide, suggesting the transformation of calcite to calcium oxide [28]. Analyzing the values of each peak given, we conclude that the phases obtained after calcination at 200, 400, 500, 600, 700, and 800°C are a mixture of two $CaCO_3$ phases with different crystalline phases aragonite, calcite, and CaO [11]. These results confirmed the previous explanation posed in visual aspects and thermal treatment and the result obtained in the differential scanning calorimeter (DSC) and Thermogravimetric analysis with Derivative thermogravimetry (DSC/TGA-DTG).

3.3 Surface analysis

3.3.1 SEM and EDXS

Figure 6. represent the morphological surfaces of *snail shell* before and after calcination at different temperatures of 200, 400, 500, 600, 700, and 800°C for 4 h. Figure 6(A-C) shows the surface of raw SSP and calcined *snail shells* at 200°C and 400°C, respectively. These surfaces have an irregular microstructure and a uniform distribution of calcium carbonate seeds with a rough surface. The observation of calcium carbonate seeds of the rod-like form indicates the existence of aragonite phases of the *orthorhombic* crystal form of $CaCO_3$ particles

[25]. Also, the formation of pores is due to dehydration during the thermal treatment [31]. The increase in temperature towards 600°C presents a uniform surface with numerous small seeds ($CaCO_3$) representing a smooth, homogeneous, and compact surface, as shown in Figure 6(D-E). This increase favours a transformation of the calcium carbonate phases from aragonite as *orthorhombic* to calcite as *rhombohedric* crystal form, respectively, which agrees with the XRD analyses [4]. The calcination of SSP at temperatures ranging from 700°C to 800°C is shown in Figure 6(F-G), and the surface becomes smoother, more homogeneous, and uniform than at other temperatures. The formation of pores releases carbon dioxide (CO_2) according to reaction R-4.

$$CaCO_{3\,(s)} \rightleftarrows CaO_{(s)} + CO_{2\,(g)} \qquad \text{R-4}$$
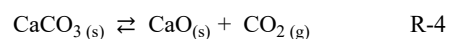
This change in morphology during the increase of the temperature is due mainly to the transformation of the phases of calcite ($CaCO_3$) to the oxides of Calcium (CaO) of the crystalline form *cubic*, which is well observed in Figure 6(G') [32]. These results confirm the emerged pic in R-XD showed the transformation of the $CaCO_3$ to CaO at a temperature of 800°C. This result was in agreement with and confirmed the obtained result of differential scanning calorimeter (DSC) and Thermogravimetric analysis with Derivative thermogravimetry (DSC/TGA-DTG) and Fourier transform-infrared spectroscopy (FT-IR) [4], [11], [25], [28].

Figure 7 shows a scanning electron spectroscopy (SEM) image of the particle sizes of SSP ground in ethanol and then calcined at 800°C. The measurement of the particle sizes is done by taking 7 particles that are shown in the image. The mechanochemical grinding process of the *snail shell* allowed us to obtain particles of micrometric size between 3311 µm to 10140 µm. Therefore, mechanochemical grinding is a process that leads to getting particles by a top-down aspect [15]. It is a destructive method that consists of going from macrometric to micrometric size. The mechanochemically prepared and heat-treated particles of SSP reinforced the polystyrene polymer. They found that the micrometre-sized particles improved

the properties of the formed PS/SSP composites with percentages ranging from 1% to 10% [14]. The mechanochemical process is a manufacturing technique of micromaterials and nanomaterials that go through a dry grinding and then the other wet, based on the principle of top-down preparation. Going from large particle size to nanometer size [7,13,15].

EDXS utilized in scanning and transmission electron microscopes provides information regarding the sample's elemental composition and is studied in the microscope using emission spectroscopy. Figure 8 shows the elemental composition of the raw SSP and SSP calcined at different temperatures of 200, 400, 500, 600, 700, and 800°C for 4 h. The major element in raw and calcined SSP was calcium (Ca), oxygen (O), and carbon (C), forming $CaCO_3$ aragonite and calcite phases. Other minor elements as Fe, Al, K, and P, with small weights [11]. Laonapakula *et al*. [28], studied the elemental composition of *Blood Cockle Shell* (BCS) and *Golden Apple Snail Shell* (GASS). They discovered that the BCS and GASS consisting of major elements (Ca, O, and C) increase with the temperature of calcination, and trace elements decrease (Na, Sr, Cl, Si, Mg, S, Fe, Al, K, Mn, P, and Ba). They confirm that the *GASS* has a higher composition of CaO, contrary to *BCS*. The same results were obtained in other literature studies [11,20,25]. The obtained result suggests that the SSP is not the pure composition of calcium carbonate due to the existence of other trace elements [20,33].
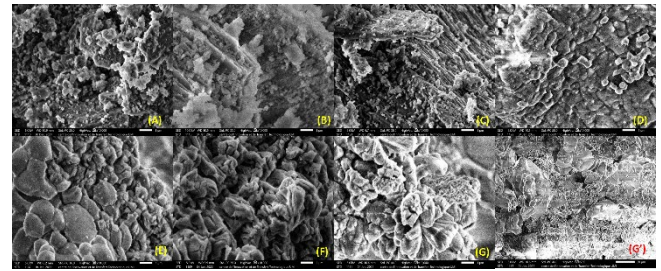

Figure 6. SEM images of: (A) raw SSP; (B) calcined SSP at 200°C, (C) calcined SSP at 400°C, (D) calcined SSP at 500°C, (E) calcined SSP at 600°C, (F) calcined SSP at 700°C, and G, G' calcined SSP at 800°C.
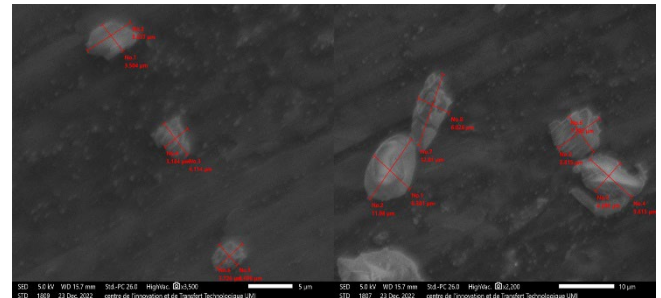

Figure 7. SEM image shows the sizes of the particles of the snail shell grounded in ethanol and calcined at 800°C.
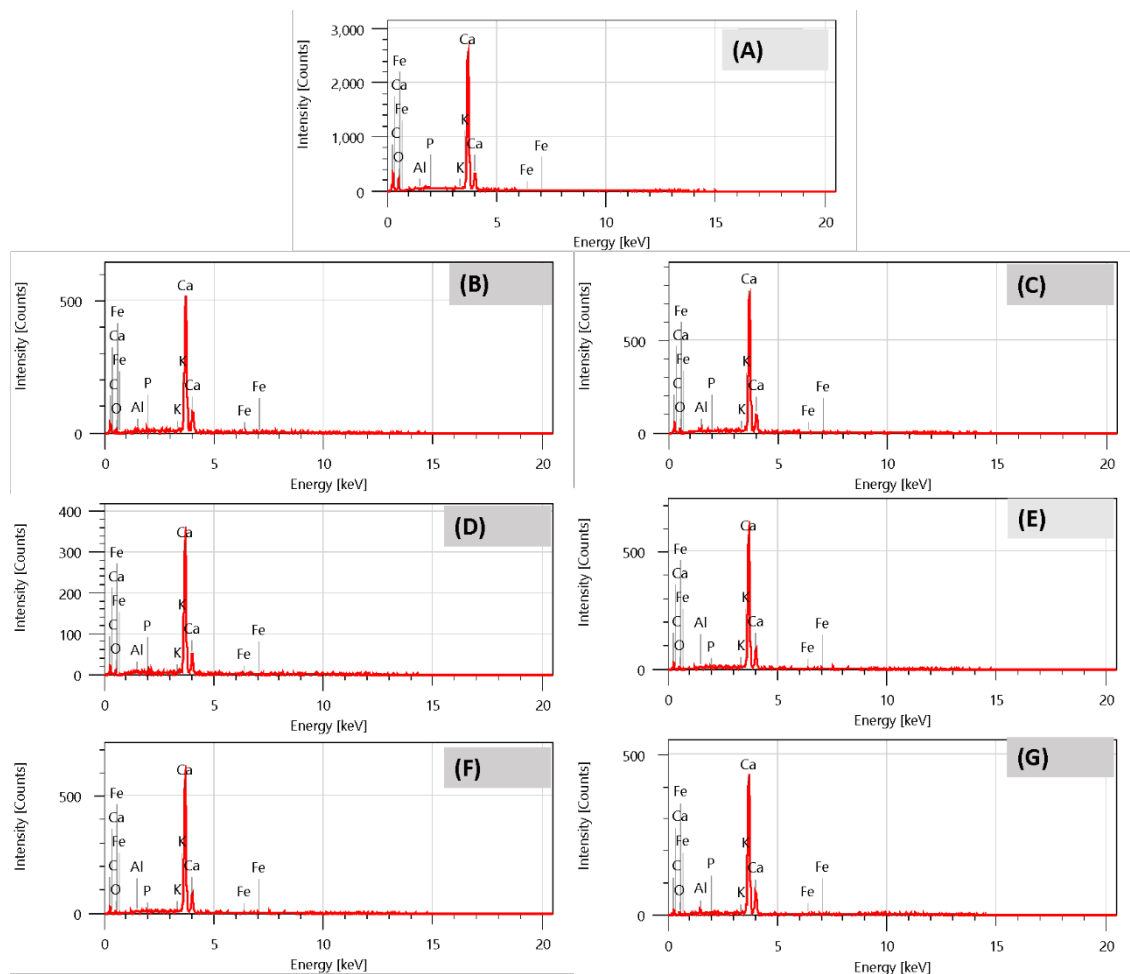

Figure 8. EDXS spectra of: A) raw SSP; (B) calcined SSP at 200°C, (C) calcined SSP at 400°C, (D) calcined SSP at 500°C, (E) calcined SSP at 600°C, (F) calcined SSP at 700°C, and G calcined SSP at 800°C.

4. Conclusion

The mechanochemical process lets us obtain SSP particles of micrometric size ranging from 3311 µm to 10140 µm. In other words, the mechanochemical process allows us to fine particles of a micrometric size that positively influence the SSP's properties. In addition, increasing their surface area and reactivity facilitates the release of water and water linked to polymorphs $CaCO_3$. Also, the transformation and decomposition of $CaCO_3$ to CaO in the *snail shell*. SEM confirms the size of *snail shell* particles and porous and smooth surfaces at 800°C. The thermal treatment affects crystalline phase transformations in SSP. The analysis of weight losses at each temperature was investigated. Thermal analysis by differential scanning calorimetry (DSC)/ Thermogravimetric TGA-DTG and X-Ray Diffraction (XRD) revealed the transformation of the crystalline phases of SSP. The aragonite phase of $CaCO_3$ was transformed into a calcite crystalline phase at 400°C to 600°C. The endothermic decomposition of the $CaCO_3$ phase to CaO occurs at temperatures above 800°C. The transformation is accompanied by a loss of about 47.79% of the initial sample weight due to CO_2 release. The weight of the SSP was constant at temperatures above 800°C. At this point, the $CaCO_3$ in the *snail shell* was partially converted to CaO. These results were confirmed by FT-IR, DSC, and XRD analyses. The SSP calcined at 700°C and 800°C has high calcium. The content of calcium increases with increasing calcination temperature. The concentration of CaO produced by the calcination of SSP is highly advantageous for various commercial applications. Hence, interesting challenges exist to develop economic materials and solutions to disposal problems, especially for the by-products of a *snail shell*.

Acknowledgements

References

[1]   J. Ihli, Y. Y. Kim, E. H. Noel, and F. C. Meldrum, "The effect of additives on amorphous calcium carbonate (ACC): Janus behavior in solution and the solid state," *Advanced Functional Materials*, vol. 23, no. 12, pp. 1575-1585, 2013.

[2]   B. Janković, I. Smičiklas, N. Manić, A. Mraković, M. Mandić, D. Veljović, and M. Jović, "Thermo-oxidative evolution and physico-chemical characterization of seashell waste for application in commercial sectors," *Thermochimica Acta*, vol. 686, p. 178568, 2020.

[3]   S. Rujitanapanich, P. Kumpapan, and P. Wanjanoi, "Synthesis of hydroxyapatite from oyster shell via precipitation," in *Energy Procedia*, vol. 56, no. C, pp. 112-117, 2014.

[4]   T. Witoon, "Characterization of calcium oxide derived from waste eggshell and its application as CO_2 sorbent," *Ceramics International*, vol. 37, no. 8, pp. 3291-3298, 2011.

[5]   M. Egerić, I. Smičiklas, A. Mrakovic, M. Jovic, M. Sljivic-Ivanovic, J. Sokolović, and M. Ristić, "Separation of Cu(II) ions from synthetic solutions and wastewater by raw and calcined seashell waste," *Desalination Water Treat*, vol. 132, pp. 205-214, 2018.

[6]   E. O. Jatto, I. O. Asia, F. Egharevba, and C. J. Ewansiha, "Kinetics studies of the treatment of wastewater from brewery industry, using powdered snail shell," *Water-Energy Nexus*, vol. 3, pp. 95-102, 2020.

[7]   O. J. Gbadeyan, S. Adali, G. Bright, and B. Sithole, "The investigation of reinforcement properties of nano-$CaCO_3$ synthesized from Achatina fulica snail shell through mechanochemical methods on epoxy nanocomposites," *Nanocomposites*, vol. 7, no. 1, pp. 79-86, 2021.

[8]   R. Bhoopathi and M. Ramesh, "Influence of eggshell nanoparticles and effect of alkalization on characterization of industrial hemp fibre reinforced epoxy composites," *Journal* of Polymers and the *Environment*, vol. 28, no. 8, pp. 2178-2190, 2020.

[9]   I. Y. Suleiman, V. S. Aigbodion, C. O. Obayi, and K. Mu'azu, "Surface characterisation, corrosion and mechanical properties of polyester-polyester/snail shell powder coatings of steel pipeline for naval applications," *International Journal of Advanced Manufacturing Technology*, vol. 101, no. 9-12, pp. 2441-2447, 2019.

[10] C. Wang, J. Zhao, X. Zhao, H. Bala, and Z. Wang, "Synthesis of nanosized calcium carbonate (aragonite) via a polyacrylamide inducing process," *Powder Technology*, vol. 163, no. 3, pp. 134-138, 2006.

[11] R. Ouafi, A. Ibrahim, I. Mehdaoui, M. Asri, M. Taleb, and Z. Rais, "Spectroscopic Analysis of chemical compounds derived from the calcination of snail shells waste at different temperatures," *Chemistry Africa*, vol. 4, no. 4, pp. 923-933, 2021.

[12] S. Parveen, A. Chakraborty, D. K. Chanda, S. Pramanik, A. Barik, and G. Aditya, "Microstructure analysis and chemical and mechanical characterization of the shells of three freshwater snails," *ACS Omega*, vol. 5, no. 40, pp. 25757-25771, 2020.

[13] O. J. Gbadeyan, S. Adali, G. Bright, B. Sithole, and S. Onwubu, "Optimization of Milling Procedures for Synthesizing Nano-$CaCO_3$ from Achatina fulica Shell through Mechanochemical Techniques," *Journal of Nanomaterials*, vol. 2020, pp. 1-9, 2020.

[14] M. Karaoui, R. Hsissou, M. Alami, and M. Assouag, "Thermal, flow, and mechanical properties of composites based on polystyrene (PS) and snail shell powder (SSP) biofiller (PS/SSP)," *Iranian Polymer Journal (English Edition)*, vol. 32, no. 4, pp. 1-11, 2023.

[15] A. Oyetunji, R. Umunakwe, B. O. Adewuyi, U. S. Nwigwe, and I. J. Umunakwe, "Evaluating the properties of nanoparticles of calcium carbonate obtained from the shells of african giant land snails (Achatina achatina) via in situ deposition technique," *UPB Scientific Bulletin, Series B: Chemistry and Materials Science*, vol. 81, no. 1, pp. 86-94, 2019.

[16] P. Maravelaki-Kalaitzaki, A. Bakolas, and A. Moropoulou, "Physico-chemical study of Cretan ancient mortars," *Cement Concrete Research*, vol. 33, no. 5, pp. 651-661, 2003.

[17] P. Maravelaki-Kalaitzaki, A. Bakolas, I. Karatasios, and V. Kilikoglou, "Hydraulic lime mortars for the restoration of historic masonry in Crete," *Cement Concrete Research*, vol. 35, no. 8, pp. 1577-1586, 2005.

[18] S. Yoshioka, and Y. Kitano, "Transformation of aragonite to calcite through heating," *Geochemical Journal,* vol. 19, no. 4, p. 245-249, 1985.

[19] A. Shafiu Kamba, M. Ismail, T. A. Tengku Ibrahim, and Z. A. B. Zakaria, "Synthesis and characterisation of calcium carbonate aragonite nanocrystals from cockle shell powder (Anadara granosa)," *Journal of Nanomaterials*, vol. 2013, no. 8, p. 5, 2013.

[20] V. Fombuena, L. Bernardi, O. Fenollar, T. Boronat, and R. Balart, "Characterization of green composites from biobased epoxy matrices and bio-fillers derived from seashell wastes," *Materials and Design*, vol. 57, pp. 168-174, 2014.

[21] S. Hu, Y. Wang, and H. Han, "Utilization of waste freshwater mussel shell as an economic catalyst for biodiesel production," *Biomass Bioenergy*, vol. 35, no. 8, pp. 3627-3635, 2011.

[22] F. Cestari, G. Chemello, A. Galotta, and V. M. Sglavo, "Low-temperature synthesis of nanometric apatite from biogenic sources," *Ceramics International*, vol. 46, no. 15, 2020.

[23] S. A. S. Bonou, E. Sagbo, C. Aubry, C. Charvillat, B. Ben-Nissan, and S. Cazalbou, "Conversion of snail shells (Achatina achatina) acclimatized in Benin to calcium phosphate for medical and engineering use," *Journal of the Australian Ceramic Society*, vol. 55, no. 4, pp. 1177-1186, 2019.

[24] Y. Kezuka, K. Kawai, K. Eguchi, and M. Tajika, "Fabrication of single-crystalline calcite needle-like particles using the aragonite-calcite phase transition," *Minerals*, vol. 7, no. 8, p. 133, 2017.

[25] D. Asmi, and A. Zulfia, "Blood cockle shells waste as renewable source for the production of biogenic CaCO$_3$ and Its characterization," in *IOP Conference Series: Earth and Environmental Science*, vol. 94, no. 1, p. 012049, 2017.

[26] C. W. Loy, K. A. Matori, W. F. Lim, S. Schmid, N. Zainuddin, Z. A. Wahab, Z. N. Alassan, and M. H. Zaid, "Effects of calcination on the crystallography and nonbiogenic aragonite formation of ark clam shell under ambient condition," *Advances in Materials Science and Engineering*, vol. 2016, no. 3-4, pp. 1-8, 2016.

[27] S. Milano, and G. Nehrke, "Microstructures in relation to temperatureinduced aragonite-To-calcite transformation in the marine gastropod Phorcus turbinatus," *Plos One Journal*, vol. 13, no. 10, 2018.

[28] T. Laonapakul, R. Sutthi, P. Chaikool, Y. Mutoh, and P. Chindaprasirt, "Optimum conditions for preparation of bio-calcium from blood cockle and golden apple snail shells and characterization," *Journal of The Science Society of Thailand*, vol. 45, no. 1, p. 10, 2019.

[29] C. S. Korach, and R. L. Pai, "Mechanical properties of a nano-tructured poly (KAMPS)/aragonite composite," *Mechanics of Biological System and Materials*, vol. 2, pp. 131-136, 2011.

[30] M. B. Toffolo, and E. Boaretto, "Nucleation of aragonite upon carbonation of calcium oxide and calcium hydroxide at ambient temperatures and pressures: A new indicator of fire-related human activities," *Journal* of *Archaeological Science*, vol. 49, no. 1, 2014.

[31] L. S. Gomez-Villalba, P. López-Arce, M. Alvarez De Buergo, and R. Fort, "Atomic defects and their relationship to aragonite-calcite transformation in portlandite nanocrystal carbonation," *Crystal Growth and Design*, vol. 12, no. 10, 2012.

[32] S. L. M. A. Ghafar, M. Z. Hussein, and Z. A. B. Zakaria, "Synthesis and characterization of cockle shell-based calcium carbonate aragonite polymorph nanoparticles with surface functionalization," *Journal* of *Nanomaterials*, vol. 2017, 2017.

[33] K. N. Islam, M. Z. B. A. Bakar, M. M. Noordin, M. Z. bin Hussein, N. S. B. A. Rahman, and M. E. Ali, "Characterisation of calcium carbonate and its polymorphs from cockle shells (Anadara granosa)," *Powder Technology*, vol. 213, no. 1, 2011.